Hindawi
Advances in Civil Engineering
Volume 2021, Article ID 6689212, 15 pages
https://doi.org/10.1155/2021/6689212

Research Article

Experimental Study on Local Scour and Related Mechanical Effects at River-Crossing Underwater Oil and Gas Pipelines

Fan Cui,[1,2,3] **Yunfei Du**,[1] **Xianjie Hao**,[2] **Suping Peng**,[1,2] **Zhuangzhuang Bao**,[1] **and Shiqi Peng**[1]

[1]*School of Geosciences and Surveying Engineering, China University of Mining and Technology, Beijing 100083, China*
[2]*State Key Laboratory of Coal Resources and Safe Mining, China University of Mining and Technology, Beijing 100083, China*
[3]*Beijing Key Laboratory for Precise Mining of Intergrown Energy and Resources, China University of Mining and Technology, Beijing 100083, China*

Correspondence should be addressed to Xianjie Hao; haoxianjie_cumtb@126.com

Received 17 December 2020; Revised 18 March 2021; Accepted 5 April 2021; Published 21 April 2021

Academic Editor: Jia Lin

Among the various geological disasters that threaten the safe operation of long-distance oil and gas pipelines, water-damage disasters are numerous and widely developed. Especially the pipelines crossing river channels or gullies are vulnerable to scouring hazards from storms and floods. A water-damage disaster physical model was established to investigate the characteristics of the riverbed scour profile and the pipeline force when the pipeline was buried at different depths under the condition of different particle size riverbed sediment. Results indicated that the equilibrium scour depth changed in a spoon shape with the gradual increase of the embedment ratio in general. The equilibrium scour depth formed by the fine sand riverbed was the largest, about 1.5 times the pipeline diameter. When the pipeline was half exposed, the clay riverbed was more resistant to the scour of the river than the riverbed of fine sand and very fine pebbles with a larger particle size. In the riverbed of three particle sizes, fine sand was more difficult to withstand the scour of the river. The scour profile formed by the sand bed around the pipeline and the force and deformation of the pipeline were related to pipeline location and riverbed sediment type. Results of this study might be useful for the safety warning and protection measures of underwater pipeline crossing.

1. Introduction

Oil and gas pipelines play an important role in the deployment of oil and natural gas resources [1]. By the end of 2017, the total mileage of global oil and gas pipelines in service was approximately 355×10^4 km, including 296.56×10^4 km for natural gas pipelines and 58.4×10^4 km for crude oil pipelines [2]. Long-distance oil and gas pipelines inevitably have to cross rivers. Two methods are generally adopted when oil and gas pipelines traverse a river: underwater crossing and water crossing. For the former, due to the effects of riverbed evolution, riverbed scour, and water current impact, the pipeline is partially suspended or exposed and is easily damaged, which increases the risk of damage to the oil and gas pipeline at the river bottom [3]. Once the oil and gas pipeline at the bottom of the river is damaged, it is very easy to cause dangerous situations such as leakage, poisoning, fire, or explosion. This not only is harmful to the environment, but also can cause serious economic losses and even endanger human life [4].

With the rapid development of oil and gas pipeline construction in various countries around the world, pipeline safety accidents caused by local scour of the pipeline have occurred from time to time [5]. For example, in 2011, ExxonMobil's Silvertip pipeline near Laurel was exposed and then ruptured due to riverbed erosion, causing pollution of miles of riverbanks. As a result, the municipal water supply and irrigation districts in eastern Montana were forced to suspend water from the river [6]. In 1994, the flooding of the San Jacinto River in Texas, USA, caused multiple pipelines to rupture, causing 34,500 barrels of crude oil and petroleum products to be discharged into the river and ignited [7].

Therefore, more and more scientific researchers have begun to pay attention to the problem of pipeline local scour. Mao [8], Sumer et al. [9–12], Chiew [13–15], Neelamani and Rao [16], Yang et al. [17], and Gao et al. [18] mainly studied the local scour process and mechanism of submarine pipeline by establishing physical models. Van Beek and Wind [19], Zhao et al. [20], and Liu et al. [21] used numerical simulation methods to study the flow field changes, bed surface pressure distribution, and pipeline surface pressure distribution during the local scour process of submarine pipelines. In addition, with the development of new technologies, some new equipment and methods have also been applied to the study of pipeline scouring. An et al. proposed a new type of contact image sensor (CIS) to track the development of scour pits near bridge piers [22]. Zhu et al. used a miniature camera installed in a transparent pipe to show the results of a visual experiment of three-dimensional scouring of the pipe [23]. Azamathulla and Zakaria [24] applied the artificial neural network (ANN) to pipeline scour depth estimation and verified the effectiveness of the method. In addition to that, they also studied the temporal variation of local pipeline scour depth to estimate the scour depth and proposed a regression model that can well predict the relative scour depth [25]. Najafzadeh et al. [26–29] applied the group method of data handling (GMDH) network method to predict the pipeline scour depth under wave action and compared the performance of this method with the adaptive neurofuzzy inference system (ANFIS) model, model tree (MT), and empirical formula, which verifies the superiority of the GMDH network in predicting the scour depth. Based on the above analysis, it is not difficult to find that there are many studies on long-distance oil and gas pipelines; nevertheless, most of those studies mainly focus on the prediction of scour depth and the calculation of critical suspended length. Besides, most researches are on the evolution process and scour characteristics of the seabed around submarine pipelines, and few studies are on local scour of oil and gas pipelines crossing rivers. In addition, different riverbed medium at different depth will inevitably lead to changes in the evolution process of scour.

Thus, a physical model of the local scour of oil and gas pipelines crossing rivers under water was established based on experimental conditions. Subsequently, the characteristics of riverbed scour profile and the stress and deformation of the pipeline when the pipeline was buried at different depths of the riverbed under the conditions of different particle sizes of riverbed sediment were studied. The major emphasis of the experiment is that we compared the characteristics of the scour profiles formed in the process of the pipeline being scoured by the river under the action of the riverbed with different particle sizes and also analyzed the pressure and strain situation of the pipeline itself in this process. This study can provide theoretical guidance for the protection engineering of oil and gas pipelines crossing rivers under water and avoid serious accidents such as pipeline explosion and leakage caused by hydraulic factors.

2. Materials and Methods

2.1. Model Design

2.1.1. Model Design Principle. Local scour of oil and gas pipelines crossing rivers will cause the riverbed around the pipelines to drop, which will seriously affect the safety of operation pipelines [30, 31]. The maximum depth of riverbed descent around the pipeline is called the equilibrium scour depth. It can be used as an indicator of the intensity of local scour. As the local scour of oil and gas pipelines across rivers involves the interaction between water flow, sediment, and pipelines, the relationship between each physical quantity and the equilibrium scour depth was established through the dimensional analysis method to explore the relationship between the physical quantities and simplify the physical equations. The physical quantities related to the scouring process of oil and gas pipelines crossing rivers are shown in Table 1.

Based on the above nine physical quantities, the scour process of oil and gas pipelines crossing rivers can be expressed as

$$f\left(u, \rho, \mu, d_{50}, \rho_s, D, g, e, S\right) = 0. \tag{1}$$

Choose u as the basic variable:

$$\begin{cases} [u] = \left[M^0 L^1 T^{-1}\right], \\ [\rho] = \left[M^1 L^{-3} T^0\right], \\ [D] = \left[M^0 L^1 T^0\right]. \end{cases} \tag{2}$$

The exponential determinant of the basic dimensions of the three basic variables u, ρ, and D is

$$\begin{vmatrix} 0 & 1 & -1 \\ 1 & -3 & 0 \\ 0 & 1 & 0 \end{vmatrix} \neq 0. \tag{3}$$

Therefore, the selected basic variables are independent of each other. According to the π theorem, the other six parameters can be expressed as the dimensionless π term as follows:

Table 1: Main physical quantities.

Attributes	Physical quantities	Symbols	Dimensions
Water flow	Flow velocity	u	LT^{-1}
	Water density	ρ	ML^{-3}
	Kinetic viscosity	μ	$ML^{-1}\cdot T^{-1}$
Sediment	Median diameter	d_{50}	L
	Sand density	ρ_s	ML^{-3}
Pipelines	Diameter	D	L
	Gravity	g	LT^{-2}
Other	Distance between the lower wall of the pipeline and the riverbed surface in the physical model	e	L
	Scour depth	S	L

$$\begin{cases} \pi_1 = \mu^{-1}\rho^1 u^1 D^1 = \dfrac{\rho u D}{\mu} = \mathrm{Re}, \\ \pi_2 = d_{50}D^{-1} = \dfrac{d_{50}}{D}, \\ \pi_3 = \rho_s\rho^{-1} = \dfrac{\rho_s}{\rho}, \\ \pi_4 = (\pi_3 - 1)g^{-1}d_{50}^{-1}u_*^2 = \dfrac{u_*^2}{(\rho_s/\rho - 1)gd_{50}} = \theta, \\ \pi_5 = eD^{-1} = \dfrac{e}{D} = G, \\ \pi_6 = SD^{-1} = \dfrac{S}{D}, \end{cases} \tag{4}$$

where Re is the Reynolds number, which represents the ratio of the inertial force to the viscous force of the fluid in the process of flowing; θ is the Shields number, which reflects the ratio of the shear stress of the water flow to the river bed sediment to the underwater weight of the sand; u_*^2 represents the friction flow rate, which can be estimated using the Colebrook–White formula [32]; G is the embedment ratio, which is the ratio of the distance between the lower wall of the pipeline and the riverbed surface in the physical model (the lower wall of the pipeline is positive when it is higher than the surface of the riverbed material, and negative if it is lower than the surface of the riverbed material) and the diameter of the pipeline.

The local scour depth of the pipeline can be expressed in a unified dimensionless form, such as

$$f\left(\frac{S}{D}, \mathrm{Re}, \frac{\rho_S}{\rho}, \frac{d_{50}}{D}, G, \theta\right) = 0, \tag{5}$$

which is

$$\frac{S}{D} = f\left(\mathrm{Re}, \frac{\rho_S}{\rho}, \frac{d_{50}}{D}, G, \theta\right). \tag{6}$$

Refer to the actual pipeline diameter and experimental conditions to choose a pipeline diameter D of 4 cm.

2.1.2. Model Sand Selection. Seven different types of sediments were selected according to the particle size: clay, fine sand, medium sand 1, medium sand 2, coarse sand, very coarse sand, and very fine pebbles. The specific particle size distribution is shown in Figure 1 and the physical properties of sediments are shown in Table 2. In addition, the grading curves of noncohesive soils are shown in Figure 2.

2.1.3. Experimental Device. The constructed local scour test system for oil and gas pipelines crossing rivers is mainly composed of three parts: circulating water tank, pipeline model, and monitoring system. The schematic diagram of the experimental device is shown in Figure 3.

(1) Circulating Water Tank. The circulating water tank is mainly composed of a water storage tank, an experimental flume, and circulation system. The water storage tank is a rectangular parallelepiped tank with a length of 900 cm, a width of 140 cm, and a height of 100 cm. The experimental flume is a rectangular concave groove (the flume cross section is rectangular) with a length of 700 cm, a width of 60 cm, and a height of 30 cm. The side wall of the flume test area is made of transparent plexiglass, which is convenient for monitoring the scouring process and depth of sediment around the pipeline. A flat water grating is installed at the

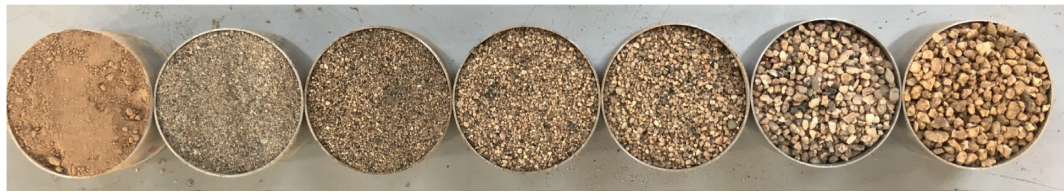

Figure 1: Test sediment.

Table 2: Physical properties of sediments.

	Clay	Fine sand	Medium sand 1	Medium sand 2	Coarse sand	Very coarse sand	Very fine pebbles
Dry density (g·cm^{-3})	1.40	1.37	1.34	1.29	1.22	1.30	1.23
Wet density (g·cm^{-3})	1.55	1.43	1.47	1.55	1.39	1.56	1.49

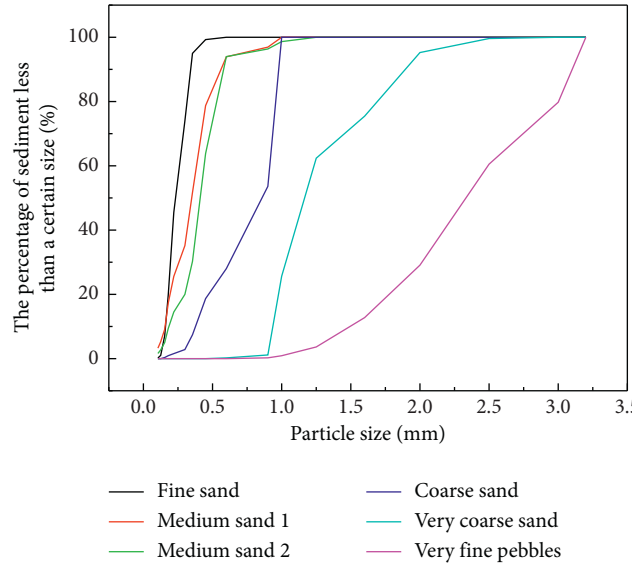

Figure 2: Grading curves.

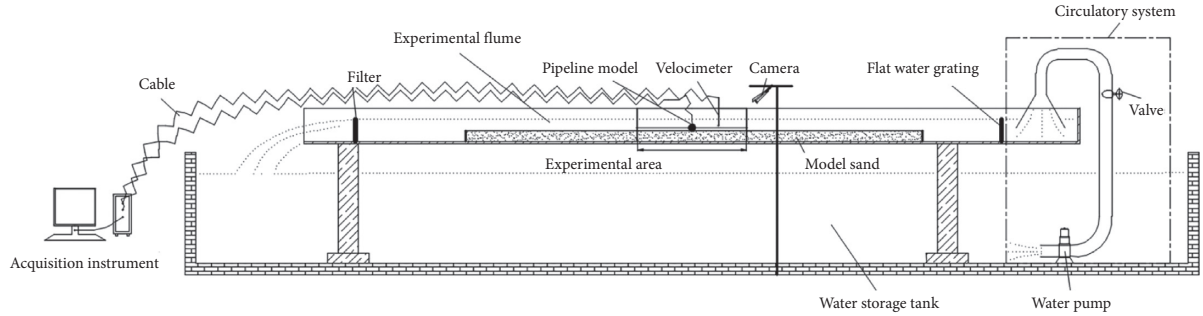

Figure 3: Schematic of the experiment.

water inlet port of the experimental flume to dissipate energy and reduce drag, so that the incoming flow is even and stable, and provides stable water flow conditions for the experiment. A filter screen is installed at the water outlet of the experimental flume to filter the model sand in the water flow to prevent the model sand from causing damage to the pump. The circulation system mainly refers to the installation of a high-power water pump at the bottom of the water storage tank and the delivery of water to the experimental flume through a water delivery pipeline. After flowing through the

experimental flume and at the end, it flows into the water storage tank again to form the water circulation.

(2) Pipeline Model. The pipeline used in the experiment is a PVC pipeline with a diameter D of 4 cm, and the pressure sensor and strain gauge are arranged on the outer surface of the central position of the pipeline axis. The specific arrangement position is shown in Figure 4. Eight pressure sensors are evenly arranged on the left profile A to monitor the pressure in the axial center section of the pipeline. Eight strain gauges are evenly arranged on the right profile B to monitor the strain in the axial center section of the pipeline.

(3) Monitoring System. As shown in Figure 5, the monitoring system consists of an Acoustic Doppler Velocimetry (ADV, type: LSH10-1M), a data acquisition instrument (type: EY221), strain gauges (type: BE120-3AA), and pressure sensors (type: HCYB-16).

2.1.4. Experimental Scheme. Seven types of riverbed sediment were designed and tested for the model performance. The length of the mobile bed is 3 m, and the length of the approaching bed is 1 m to allow the water flow to develop fully. The sediment transport along the approaching bed will not affect the scouring process of the local riverbed sediment in the pipeline. Seven groups of tests were carried out for each type of bed sediment with embedment ratios G of −2, −1.5, −1, −0.5, 0, 0.5, and 1, respectively. A total of 49 groups of experiments were conducted. Each group of experiments is carried out under live-bed condition. The schematic diagram of different embedment ratio tests is shown in Figure 6, and the test conditions of each group are shown in Table 3. Since our main concern in this experiment is the impact of riverbed particle size and pipeline depth on the riverbed scour process, it is not intended to predict the various values of riverbed scour to establish a connection with the actual project. Therefore, we ignore the influence of the sidewall effects. The experimental process is as follows:

(1) Spread the sand evenly on the bottom of the experimental flume, and the thickness of the sand is about 10 cm. Then turn on the pump to make the water flow and turn off the pump when the sediment is fully saturated.

(2) Paste the pressure sensor and strain gauge on the outer surface of the pipeline at the axial center position. Then glue two suction cups on both ends of the pipeline. The suction cups at both ends of the pipeline are adsorbed on the transparent plexiglass on the side wall of the test area of the sink to fix the pipeline. The relative position of the pipeline is determined according to the test group. After that, smooth the surface of the sand and keep the height at 10 cm.

(3) Turn on the water pump again. At the same time, the camera, data acquisition instrument, and ADV were turned on to monitor the experimental process, the force and deformation of the pipeline surface, and the water flow velocity. In order to reduce the pulsation of the water flow itself and the error caused by the monitoring process, the water flow velocity under all working conditions is averaged to $V = 0.4$ m/s, which is used as the water flow velocity in the experiment. The approach flow depth is 25 cm.

(4) When the shape of the scour hole at the bottom of the pipeline remains basically unchanged and the measured data does not change more than 1 mm for three consecutive times, it is considered that the scouring has reached equilibrium and a set of tests is done. The duration of each run is not fixed until it reaches the equilibrium scour conditions. Turn off the water pump, camera, data acquisition instrument and ADV. Then reset the type of sediment and the relative position of the pipeline according to the test groups and repeat the above steps.

3. Results

3.1. Characteristics of Equilibrium Scour Depth. The depths of the scour holes formed when each group of scouring reaches equilibrium were analyzed. The result is shown in Figure 7. It can be seen from Figure 7 that the equilibrium scour depth changed with the gradual increase of the embedment ratio in a scoop shape in general. When the embedment ratios were −2.0, −1.5, and −1.0, no scour holes were formed under the pipelines on the riverbed conditions of different particle sizes. At this time, the pipeline was buried in the riverbed and was not influenced by the river scour. When the embedment ratio was −0.5, scouring holes began to appear under the pipeline on the conditions of riverbed with other particle sizes except for the clay riverbed. The maximum depth of the scour hole formed by the fine sand riverbed was 6 cm, which was about 1.5 times the pipeline diameter. The minimum depth of the scour hole formed by the very fine pebble riverbed was 3 cm, which was about 0.75 times the pipeline diameter.

Take $G = -0.5$ as an example to study the local scour process around the pipeline. At this embedment ratio, the pipeline is half buried and half exposed. Observation of the local scour form of the sandy riverbed below the pipeline shows that the local scour of the pipeline generally goes through four stages of scour start-up, micropore formation, scour extension, and scour equilibrium. It can be seen from Figure 8 that during the scour start-up stage (Figure 8(a)), a large-scale scour hole gradually appeared behind the pipeline, the length was about 3-4 times the pipeline diameter, and the maximum depth was about 0.5 times the pipeline diameter. At the stage of micropore formation (Figure 8(b)), the back-flow surface of the pipeline near the pipeline bottom began to spray sand and water mixture as the scouring continued. Finally, a connecting gap penetrated through the bottom of the pipeline. A large amount of water-sand mixture quickly passed through the communicating gap and covered and filled with the scour hole formed in the first stage. This phenomenon is mainly caused by the seepage force generated inside the riverbed under the action of the pressure difference on both sides of the pipeline. During the

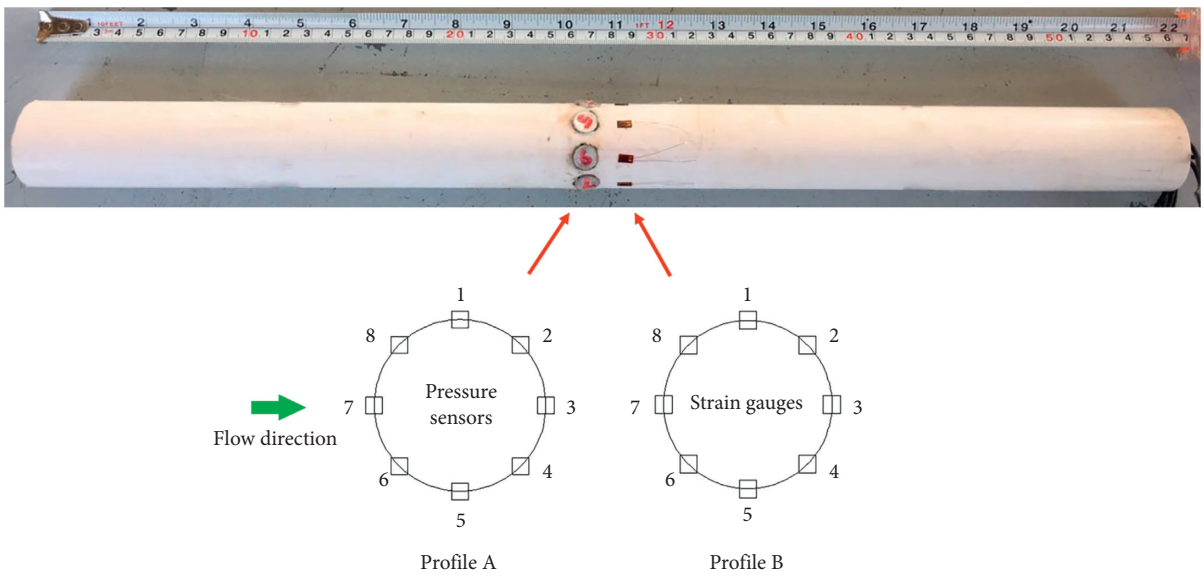

Figure 4: Schematic diagram of pipeline model sensor layout.

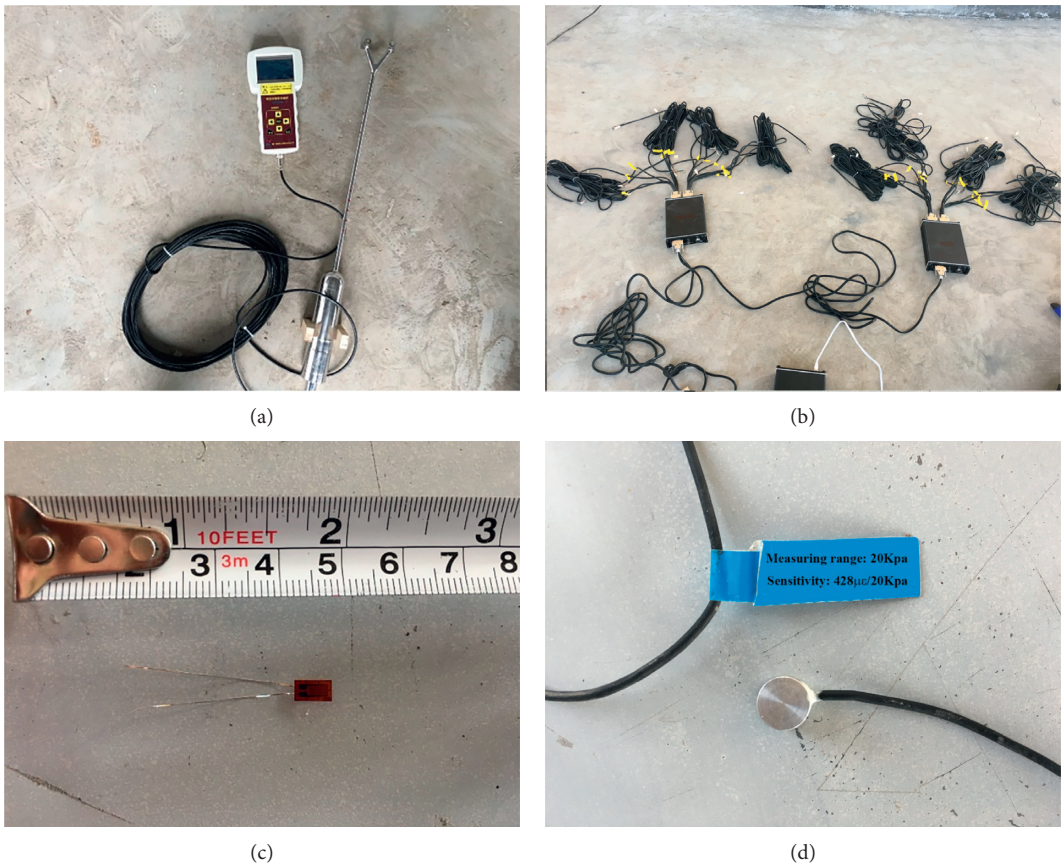

Figure 5: Physical image of the monitoring system: (a) acoustic Doppler velocimetry, (b) data acquisition unit, (c) strain gauge, and (d) pressure sensor.

stage of scour extension (Figure 8(c)), the connecting gap at the bottom of the pipeline gradually became deeper, and the speed of the water-sand mixture in the connecting gap gradually slowed down. In the scour equilibrium stage (Figure 8(d)), the shape of the scouring hole at the bottom of the pipeline basically stabilized and no longer changed.

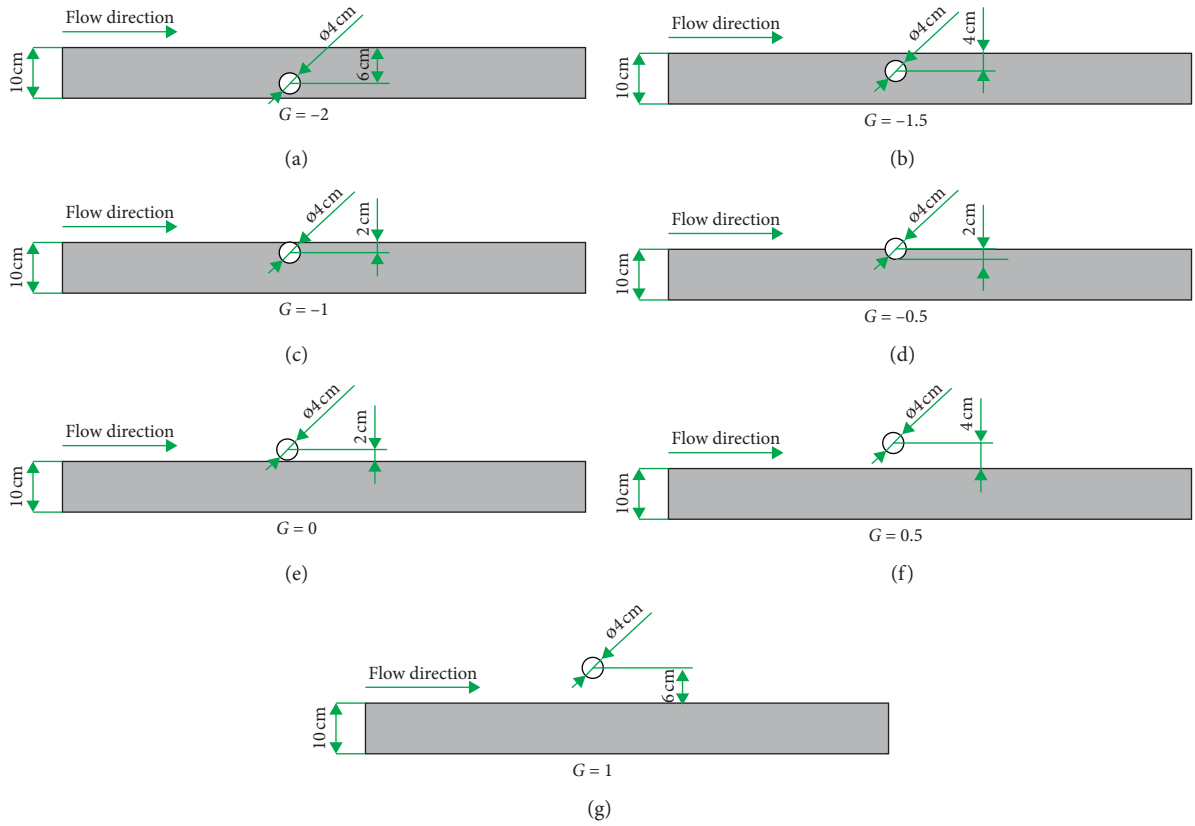

Figure 6: Schematic diagram of different embedment ratio tests: (a) schematic diagram of the test setup when the embedment ratio is −2, (b) schematic diagram of the test setup when the embedment ratio is −1.5, (c) schematic diagram of the test setup when the gap ratio is −1, (d) schematic diagram of the test setup when the embedment ratio is −0.5, (e) schematic diagram of the test setup when the embedment ratio is 0, (f) schematic diagram of the test setup when the embedment ratio is 0.5, and (g) schematic diagram of the test setup when the embedment ratio is 1.

Table 3: Test conditions.

Embedment ratio (G)	Clay		Fine sand		Medium sand 1		Medium sand 2	
	Test groups	Flow velocity ($m \cdot s^{-1}$)	Test groups	Flow velocity ($m \cdot s^{-1}$)	Test groups	Flow velocity ($m \cdot s^{-1}$)	Test groups	Flow velocity ($m \cdot s^{-1}$)
−2	1–1	0.408	2–1	0.383	3–1	0.417	4–1	0.413
−1.5	1–2	0.429	2–2	0.385	3–2	0.432	4–2	0.397
−1	1–3	0.417	2–3	0.419	3–3	0.385	4–3	0.398
−0.5	1–4	0.396	2–4	0.405	3–4	0.398	4–4	0.389
0	1–5	0.394	2–5	0.408	3–5	0.411	4–5	0.387
0.5	1–6	0.423	2–6	0.391	3–6	0.413	4–6	0.397
1	1–7	0.398	2–7	0.407	3–7	0.399	4–7	0.419
Embedment ratio (G)	Coarse sand		Very coarse sand		Very fine pebble			
	Test groups	Flow velocity ($m \cdot s^{-1}$)	Test groups	Flow velocity ($m \cdot s^{-1}$)	Test groups	Flow velocity ($m \cdot s^{-1}$)		
−2	5–1	0.384	6–1	0.398	7–1	0.395		
−1.5	5–2	0.384	6–2	0.423	7–2	0.422		
−1	5–3	0.397	6–3	0.392	7–3	0.397		
−0.5	5–4	0.391	6–4	0.423	7–4	0.395		
0	5–5	0.416	6–5	0.387	7–5	0.387		
0.5	5–6	0.385	6–6	0.404	7–6	0.414		
1	5–7	0.411	6–7	0.406	7–7	0.404		

3.2. Scour Profile Characteristics. Select representative scour profiles of clay, fine sand, and very fine pebbles under different embedment ratios for analysis, and the results are shown in Figure 9.

It can be seen from Figure 9 that under the condition of the riverbed with clay particles, when G was −2, −1.5, and −1, the pipeline was buried under the riverbed, and the bed surface was basically unchanged after the scour process. When G was −0.5, the pipeline is semiexposed to the riverbed surface. The bed surface near the pipeline area dropped by about 1.5 cm, but no through scouring holes were formed. When G was 0, 0.5, and 1 respectively, the

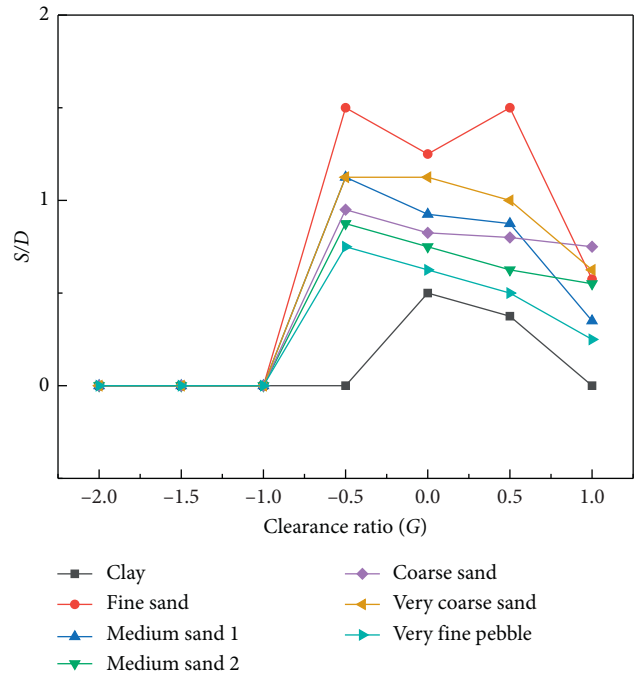

Figure 7: Variation of equilibrium scour depth with embedment ratio under different particle size riverbed conditions.

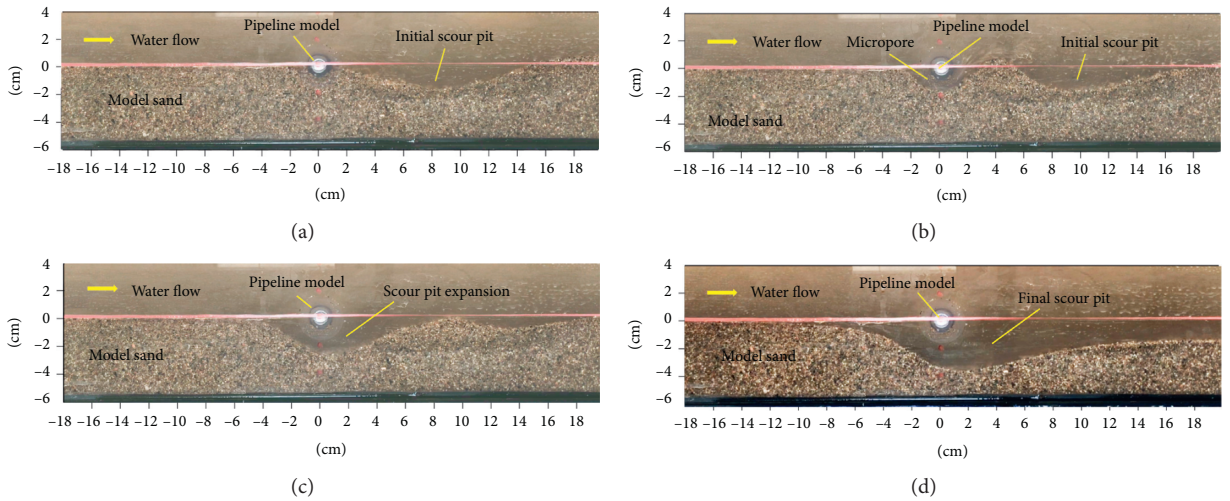

Figure 8: Local scour process around sandy riverbed pipelines: (a) scour start-up stage, (b) micropore formation stage, (c) scour extension stage, and (d) scour equilibrium stage.

pipeline was completely exposed above the riverbed, and a scour hole about 1.5 cm deep was formed at the bottom of the pipeline. Under the condition that the riverbed was constituted with fine sand, when G was −2, −1.5, and −1 respectively, the pipeline was buried under the riverbed. The entire bed surface dropped about 1 cm after scouring. When G was −0.5, 0, 0.5, and 1, the pipeline was exposed on the bed surface. After scouring, the depth of the scouring hole at the bottom of the pipeline was 4.7 cm, 4.2 cm, 3.5 cm, and 1.6 cm in sequence. The whole bed surface was lowered by about 1 cm. Under the condition that the riverbed was very fine pebble, when G was −2, −1.5, and −1 respectively, the pipeline was buried under the riverbed, and the surface of the bed was basically unchanged after scouring. When G was −0.5, 0, 0.5, and 1, the pipeline was exposed on the bed surface. After scouring, the depth of the scouring hole at the bottom of the pipeline was 2.8 cm, 2.4 cm, 1.6 cm, and 0.6 cm in sequence.

3.3. Mechanical Effect of Pipeline. The profile pressure and the strain at the axial center of the pipeline were monitored

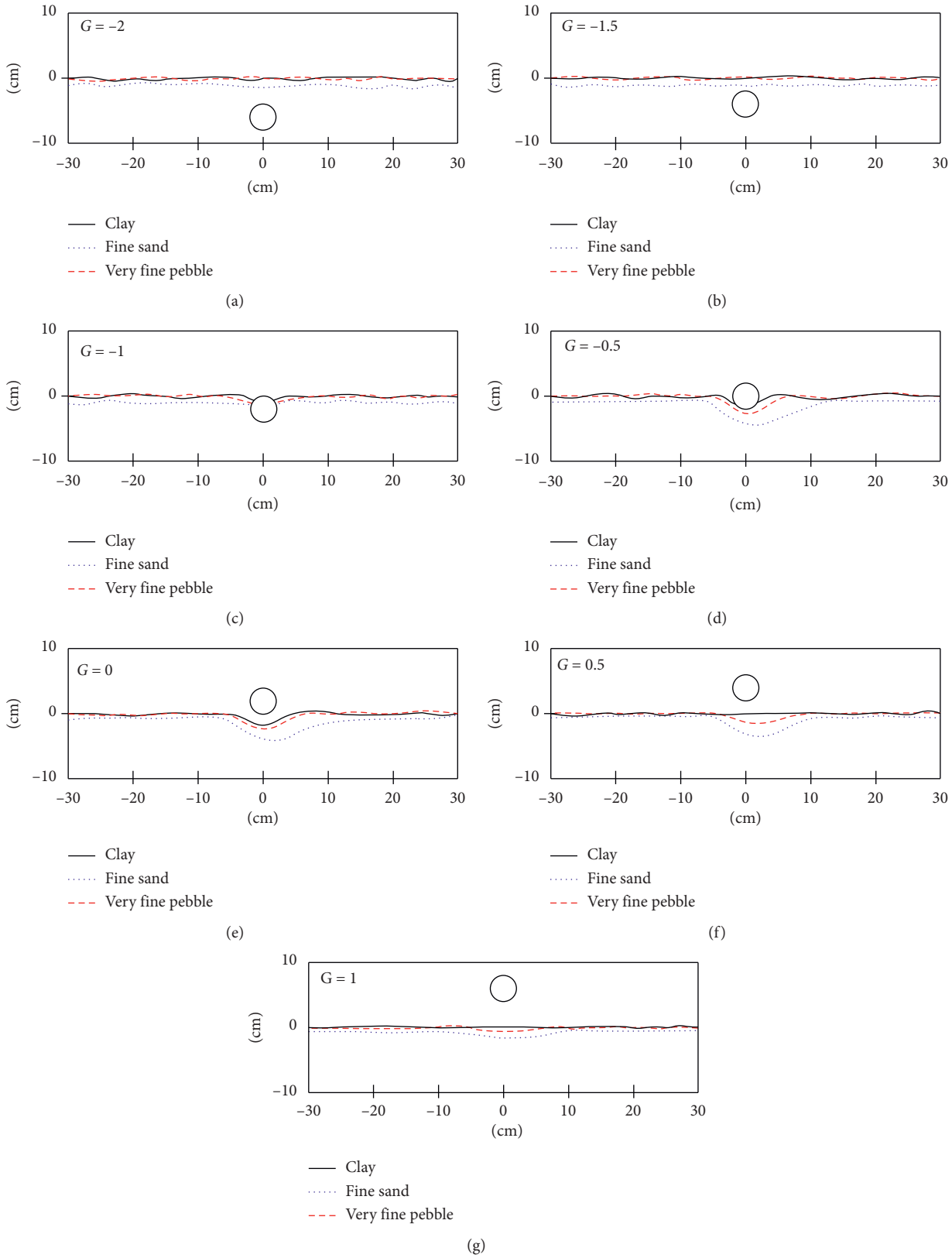

Figure 9: Scour profile under different embedment ratios: (a) scour profile with a embedment ratio of −2, (b) scour profile with a embedment ratio of −1.5, (c) scour profile with a embedment ratio of −1, (d) scour profile with a embedment ratio of −0.5, (e) scour profile with a embedment ratio of 0, (f) scour profile with a embedment ratio of 0.5, and (g) scour profile with a embedment ratio of 1.

under different embedment ratios (buried under the bed material, half buried and half exposed, and suspended on the bed material) when the bed sediments were clay, fine sand, and very fine pebble. The results are shown in Figures 10–12, respectively. The pressure and strain in Figures 10–12 refer to the measured values when the scouring reaches an equilibrium state.

Figure 10 shows the pressure and the strain on the surface of the pipeline when G was −2, −1.5, and −1 (the pipeline was buried under the riverbed as a whole). It can be seen from Figure 10 that the pressure at the top of the pipeline was greater than the pressure at the bottom of the pipeline when the sediment was clay particles. And the strain at the top of the pipeline was negative, which was in the compression zone; the strain at the bottom of the pipeline was positive, and it was in the tension zone. When the sediment was fine sand and very fine pebble, the pressure at the bottom of the pipeline was larger than that at the top of the pipeline. The strain at the bottom of the pipeline was negative, which was in the compression zone, while the strain at the top of the pipeline was positive and in the tensile zone.

Figure 11 shows the pressure and strain on the surface of the pipeline when G was −0.5 (the pipeline was half buried and half exposed). It can be seen from Figure 11 that when the sediment was clay, the pressure at the top of the pipeline was larger than that at the bottom of the pipeline. The strain at the top of the pipeline was negative, which was in the compression zone, while the strain at the bottom of the pipeline was positive, which was in the tensile zone. When the sediment was fine sand or very fine pebble, the pressure on the upstream surface of the pipeline was larger than that on the downstream surface. The upstream surface of the pipeline was strained to be negative and was in the compression zone. The strain on the downstream surface of the pipeline was positive and was in the tensile zone.

Figure 12 shows the pressure and strain on the surface of the pipeline when G is 0, 0.5, and 1, respectively (the pipeline is suspended on the riverbed). As Figure 12 shows, since the pipeline was suspended on the riverbed, the sediment type of the riverbed had little effect on the stress of the pipeline. Due to the impact of the water flow, the pressure on the upstream surface of the pipeline was greater than that on the downstream surface. The strain on the upstream surface was negative and in the compression zone, while the strain on the downstream surface was positive and in the tensile zone. It shows that the pipeline has a tendency to bend downstream at this time.

4. Discussion

When the embedment ratio was 0, scour holes appeared in the clay riverbed. The depth was 2 cm, which was about half of the pipeline diameter. But it was still less than the depth of the scour hole formed by the very fine pebble riverbed when the embedment ratio was −0.5. This is mainly due to the fact that when the noncohesive sediment starts to scour, it is mainly affected by the force of the water current (including shear stress and lifting force) and its own effective gravity. In addition to the above two forces, the cohesive sediment is also affected by the cohesive force between particles. Cohesive sediment due to the cementation between the particles causes the clay particles to require greater water flow shear stress when starting, so when the buried depth of the pipeline is changed, the scour pits appear lagging behind the noncohesive sediment bed. After that, with the gradual increase of the embedment ratio, the equilibrium scour depth under the conditions of different particle diameters of riverbeds showed a gradual decrease in general. The reason may be that as the buried depth of the pipeline decreases, the pipeline is gradually exposed to the water flow, and the eddy effect generated by the water flowing through the pipeline gradually increases. When the pipeline is completely exposed on the riverbed, the influence of the eddy effect on the riverbed sediment gradually decreases as the gap between the pipeline and the riverbed increases.

It can be seen that when G was −2, −1.5, and −1, the bed surface of the riverbed sediment with different particle sizes was basically unchanged after the scour process. It is explained that when the pipeline is buried under the riverbed, the riverbed particle size has little influence on the formation of scour holes near the pipeline. At this point, the pipeline is in a state of being less affected by the flow. When G was −0.5, the bed surface of the clay riverbed near the pipeline area dropped by about 1.5 cm. However, no through scouring holes were formed, and scouring holes with depths of 4.7 cm and 2.8 cm appeared in both the fine sand and very fine pebble riverbeds. This shows that the clay bed is more resistant to the river erosion than the fine sand and very fine pebble riverbed with larger particle size when the pipeline is semiexposed. In these three grain-size riverbeds, fine sand is more difficult to resist the river's flushing and more likely to form a larger range of scouring holes.

When G was 0, 0.5, and 1, the pipeline was completely exposed on the bed surface. At this time, a 1.5 cm deep scour hole was formed at the bottom of the pipeline in the clay riverbed. The depths of the scour holes formed by the fine sand riverbed were 4.2 cm, 3.5 cm, and 1.6 cm, respectively, and the scour holes formed by the very fine pebble riverbed were 2.4 cm, 1.6 cm, and 0.6 cm, respectively. It shows that the depth of scour hole in clay bed does not change significantly with the increase of embedment ratio when the pipeline is completely exposed to the bed. However, the depth of scour holes in fine sand and very fine pebble riverbed gradually decreases with the increase of the embedment ratio. But in general, the depth of scour holes formed by fine sand bed is greater than that of fine pebble bed.

Based on the results of Figures 10–12, it can be judged that when the pipeline is buried under the riverbed material and the sediment is clay, the pipeline has a downward bending trend, and when the sediment is fine sand or very fine pebble, the pipeline has the tendency of upward bulge. When the pipeline is half buried and half exposed and the sand is clay particles, the pipeline has a downward bending trend. When the sediment is fine sand and very fine pebbles, the pipeline tends to bend downstream.

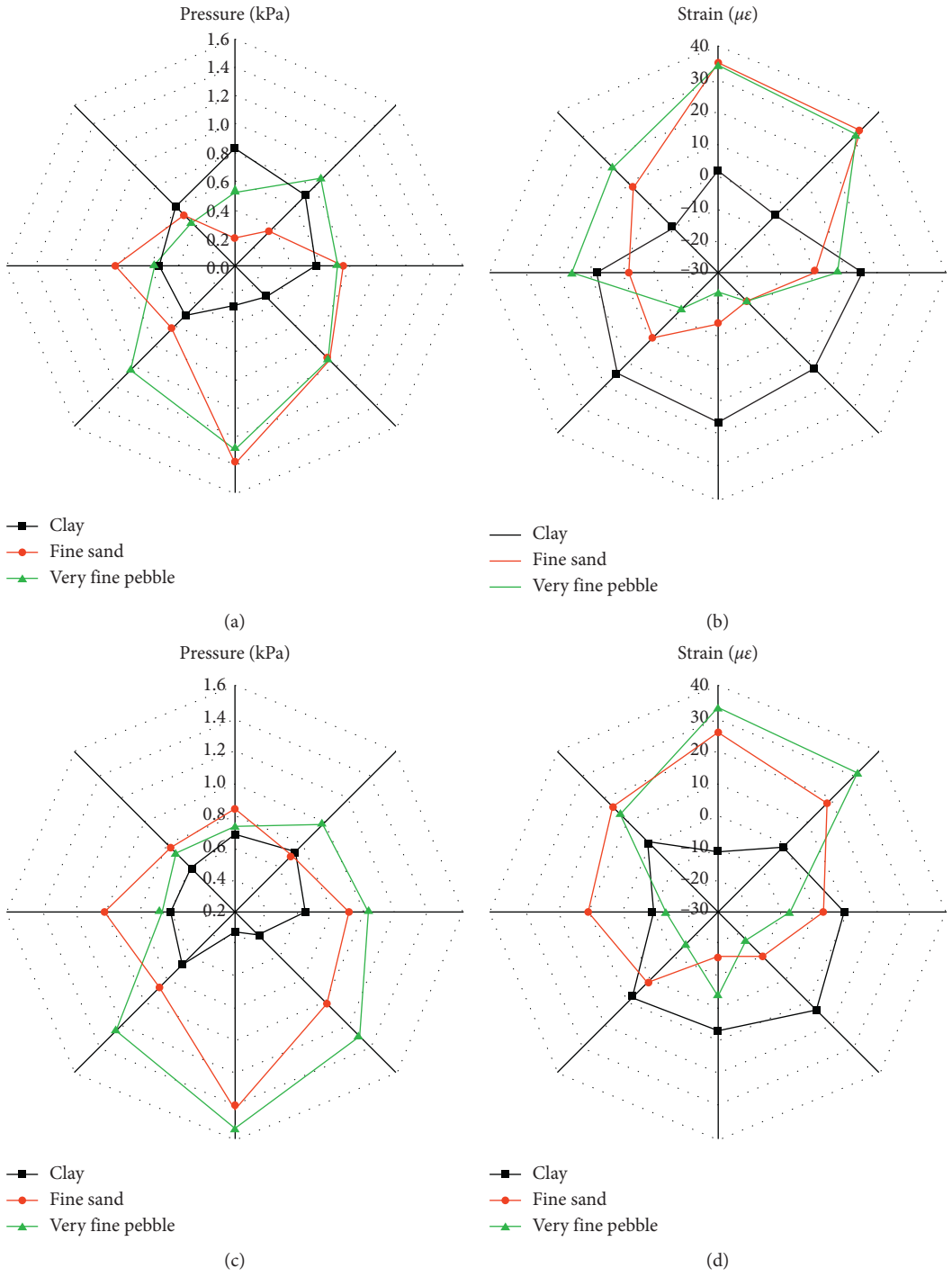

Figure 10: Continued.

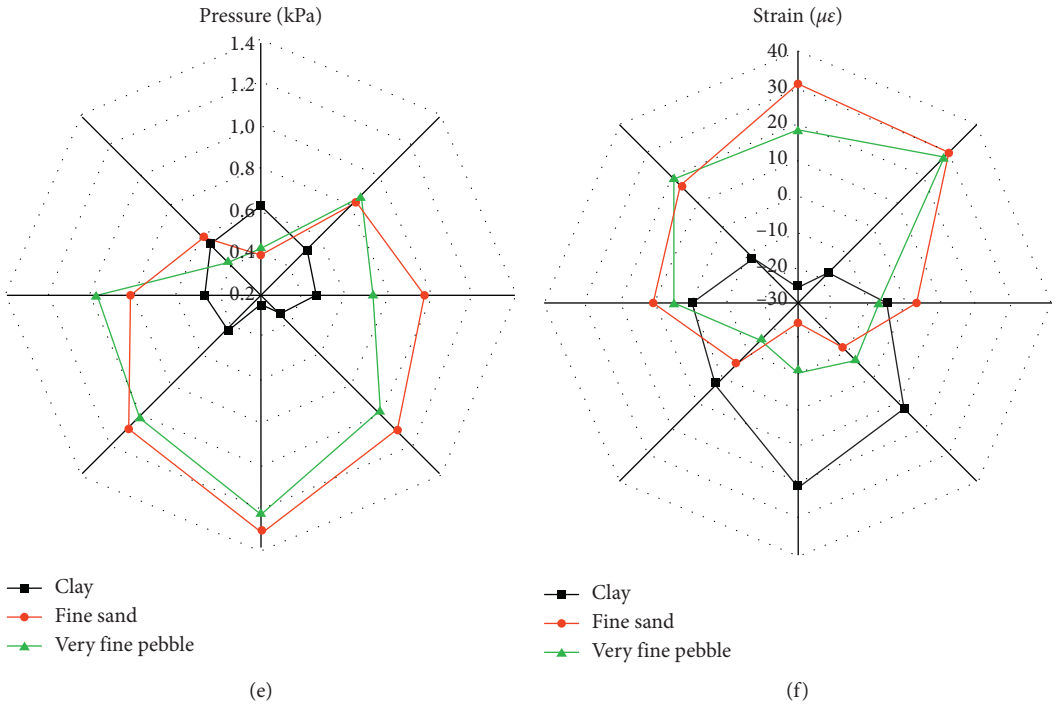

Figure 10: Pressure and strain on the surface of the pipeline which is buried under the riverbed: (a) pressure on the surface of the pipeline when the embedment ratio is −2, (b) strain on the surface of the pipeline when the embedment ratio is −2, (c) pressure on the surface of the pipeline when the embedment ratio is −1.5, (d) strain on the surface of the pipeline when the embedment ratio is −1.5, (e) pressure on the surface of the pipeline when the embedment ratio is −1, and (f) srain on the surface of the pipeline when the embedment ratio is −1.

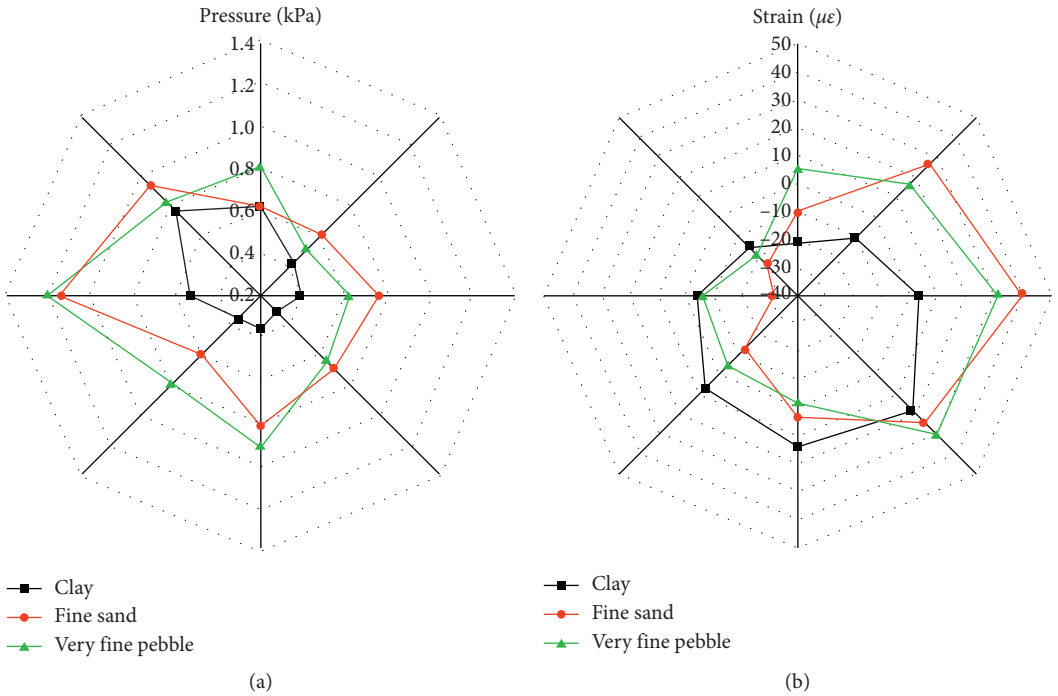

Figure 11: Pressure and strain on the surface of the pipeline when half of the pipeline is buried and half exposed: (a) pressure on the surface of the pipeline when the embedment ratio is −0.5 and (b) strain on the surface of the pipeline when the embedment ratio is −0.5.

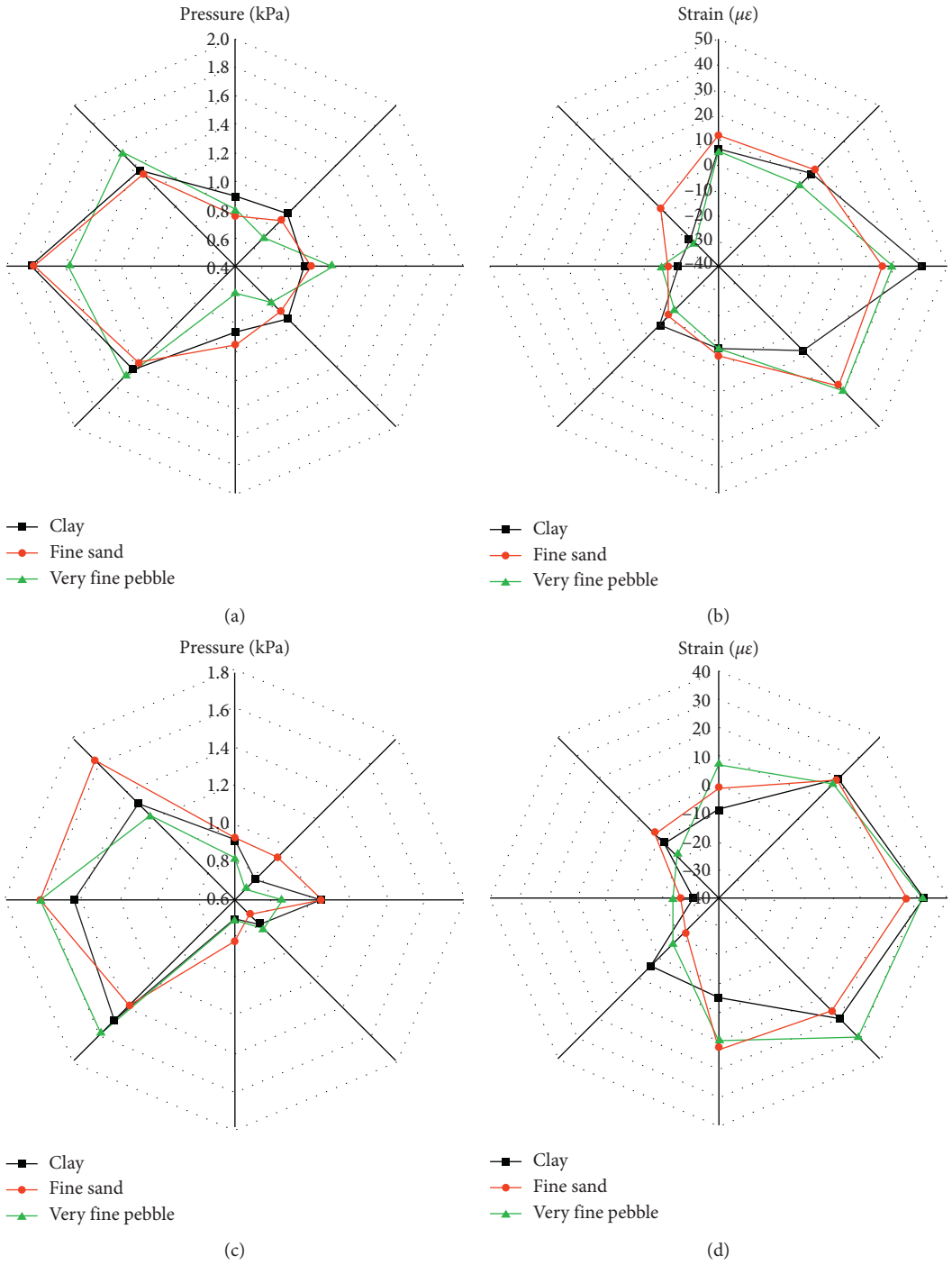

Figure 12: Continued.

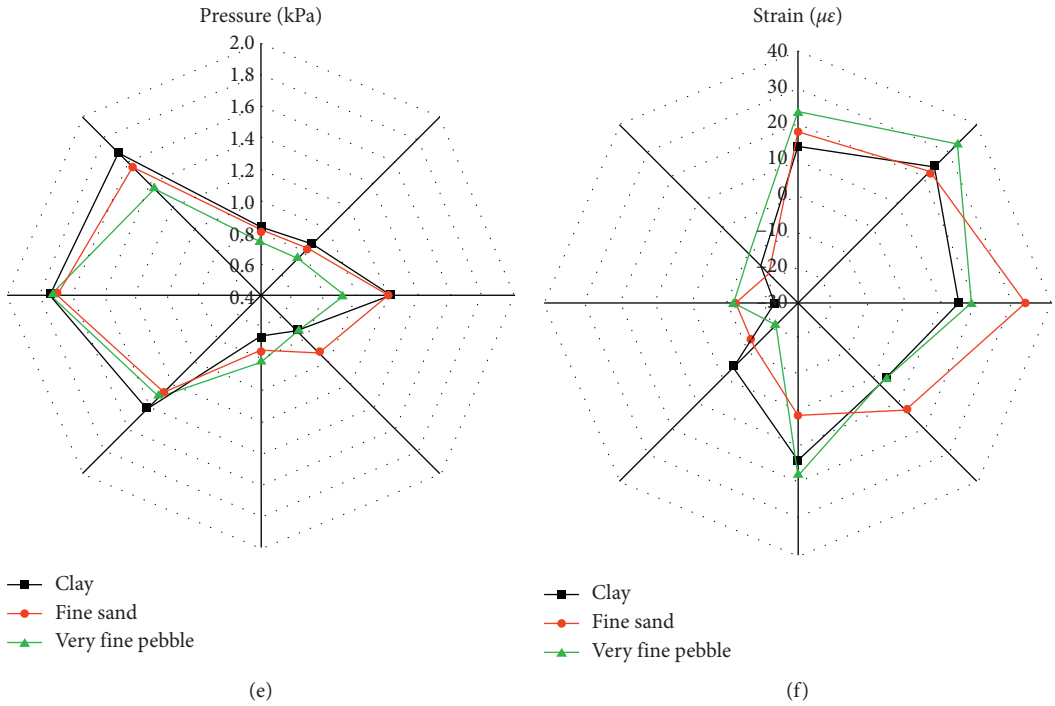

Figure 12: Pressure and strain on the surface of the pipeline which is suspended on the riverbed: (a) pressure on the surface of the pipeline when the embedment ratio is 0, (b) strain on the surface of the pipeline when the embedment ratio is 0, (c) pressure on the surface of the pipeline when the embedment ratio is 0.5, (d) strain on the surface of the pipeline when the embedment ratio is 0.5, (e) pressure on the surface of the pipeline when the embedment ratio is 1, and (f) strain on the surface of the pipeline when the embedment ratio is 1.

5. Conclusions

In this work, a physical model of water-damage disaster was established to test the characteristics of the riverbed scour profile and the pipeline force when the pipeline was buried at different depths under the condition of different particle size riverbed sediment. The following conclusions are obtained:

(a) The local scour of the pipeline generally goes through the four stages of scour start-up, micropore formation, scour expansion, and scour equilibrium. In general, the equilibrium scour depth changes in a spoon shape with the gradual increase of the embedment ratio. The equilibrium scour depth formed by fine sand riverbed is the largest, about 1.5 times of the pipeline diameter, and the clay riverbed is the smallest, about 0.5 times of pipeline diameter.

(b) When the pipeline is buried under the riverbed, the particle size of the riverbed has little effect on the formation of scour holes on the bed surface near the pipeline. When the pipeline is half exposed, the clay riverbed is more resistant to the erosion of the river than the riverbed of fine sand and very fine pebbles with a larger particle size. However, in the riverbed with three kinds of grain size, the fine sand riverbed is more likely to form a large range of scour holes. When the pipeline is completely exposed on the riverbed surface, the balance scour depth of the fine sand and very fine pebble riverbed will gradually decrease with the increase of the embedment ratio. But from the overall perspective, the equilibrium scour depth of fine sand riverbed is greater than that of very fine pebble riverbed.

(c) When the pipeline is completely buried in the riverbed, the pipeline in the clay riverbed tends to bend downward, and the pipeline in the fine sand and very fine pebble riverbed tends to uplift upward. When half of the pipeline is under the surface of the riverbed, the clay riverbed pipeline has a downward bending trend, and the fine sand and very fine pebble riverbed pipelines have a downstream bending trend. When the pipeline is completely above the surface of the riverbed, the type of riverbed sediment has little effect on the force of the pipeline. In future studies, related numerical simulation tests will be considered to explore the factors affecting the evolution of the riverbed near the pipeline. Further designs related to prototype tests are needed and they should be compared with current research works in order to improve the existing research results.

Data Availability

The data used to support the findings of this study are available from the corresponding author upon request.

Conflicts of Interest

The authors declare no potential conflicts of interest with respect to the research, authorship, and/or publication of this article.

Acknowledgments

The project was financially supported by the Major Project of Shaanxi Coal and Chemical Industry Group Co., Ltd.: Protection and Utilization of Water Resources & Research and Demonstration of Key Technologies for Ecological Reconstruction in Northern Shaanxi Coal Mining Area (2018SMHKJ-A-J-03) and the 2030 Pilot Project of CHN ENERGY Investment Group Co., Ltd.: Research on Ecological Restoration and Protection of Coal Base in Arid Ecofragile Region (GJNY2030XDXM-19-03.2).

References

[1] J. Chu, L. Yang, Y. Liu et al., "Pressure pulse wave attenuation model coupling waveform distortion and viscous dissipation for blockage detection in pipeline," *Energy Science & Engineering*, vol. 8, no. 1, pp. 260–265, 2020.

[2] H. Lu, T. Iseley, S. Behbahani, and L. Fu, "Leakage detection techniques for oil and gas pipelines: state-of-the-art," *Tunnelling and Underground Space Technology*, vol. 98, p. 103249, 2020.

[3] Q. Yang, Q. Yang, J. Yao, Y. Zhang, and Z. Wang, "Experimental study in expansion law of scour hole of pipeline crossing mountain river," *Mountain Research*, vol. 38, no. 2, pp. 241–251, 2020.

[4] Q. Li, X. Ban, and H. Wu, "Design of informationized operation and maintenance system for long-distance oil and gas pipelines," in *Proceedings of the 3rd International Conference on Computer Science and Application Engineering*, pp. 1–5, Sanya, China, 2019.

[5] X. Wang and J. Shuai, "Stress analysis of pipeline floating in flood," *Engineering Mechanics*, vol. 28, no. 2, pp. 212–216, 2011.

[6] Atkins, "Yellowstone river pipeline risk assessment and floodplain reclamation planning project," Final Report to the Yellowstone River Conservation District Council, Atkins, Epsom, UK, 2012.

[7] S. Girgin and E. Krausmann, "Historical analysis of U.S. onshore hazardous liquid pipeline accidents triggered by natural hazards," *Journal of Loss Prevention in the Process Industries*, vol. 40, pp. 578–590, 2016.

[8] Y. Mao, "The interaction between a pipeline and an erodible bed," *Febs Letters*, vol. 225, no. 1-2, pp. 218–222, 1987.

[9] B. M. Sumer and J. Fredsoe, "Onset of scour below a pipeline exposed to waves," *International Journal of Offshore and Polar Engineering*, vol. 1, no. 3, pp. 189–194, 1991.

[10] B. M. Sumer, C. Truelsen, T. Sichmann, and J. Fredsøe, "Onset of scour below pipelines and self-burial," *Coastal Engineering*, vol. 42, no. 4, pp. 313–335, 2001.

[11] B. M. Sumer, *The Mechanics of Scour in the Marine Environment*, World Scientific Publishing Company, London, UK, 2002.

[12] B. M. Sumer and J. Fredsøe, "Scour below pipelines in waves," *Journal of Waterway, Port, Coastal, and Ocean Engineering*, vol. 116, no. 3, pp. 307–323, 1990.

[13] Y. M. Chiew, "Effect of spoilers on wave-induced scour at submarine pipelines," *Journal of Waterway, Port, Coastal, and Ocean Engineering*, vol. 119, no. 4, pp. 417–428, 1993.

[14] Y. M. Chiew, "Prediction of maximum scour depth at submarine pipelines," *Journal of Hydraulic Engineering*, vol. 117, no. 4, pp. 452–466, 1991.

[15] Y. M. Chiew, "Mechanics of local scour around submarine pipelines," *Journal of Hydraulic Engineering*, vol. 116, no. 4, pp. 515–529, 1990.

[16] S. Neelamani and S. N. Rao, "Wave pressures and uplift forces on and scour around submarine pipeline in clayey soil," *Ocean Engineering*, vol. 30, no. 2, pp. 271–295, 2003.

[17] B. Yang, F. P. Gao, and Y. X. Wu, "Experimental study on local scour of sandy seabed under submarine pipeline in unidirectional currents," *Engineering Mechanics*, vol. 25, no. 3, pp. 206–210, 2008.

[18] F. Gao, X. Gu, and Q. Pu, "Experimental research on the instability process of submarine pipelines," *Chinese Journal of Geotechnical Engineering*, vol. 22, no. 3, pp. 304–308, 2000.

[19] F. A. Van Beek and H. G. Wind, "Numerical modelling of erosion and sedimentation around offshore pipelines," *Coastal Engineering*, vol. 14, no. 2, pp. 107–128, 1990.

[20] M. Zhao, S. Vaidya, Q. Zhang, and L. Cheng, "Local scour around two pipelines in tandem in steady current," *Coastal Engineering*, vol. 98, pp. 1–15, 2015.

[21] Y. Liu, H. Wang, and M. Wang, "Numerical simulation analysis of local scour around submarine pipeline," *Journal of China University of Petroleum*, vol. 36, no. 6, pp. 118–122, 2012.

[22] H. An, W. Yao, L. Cheng et al., "Detecting local scour using contact image sensors," *Journal of Hydraulic Engineering*, vol. 143, no. 4, Article ID 04016100, 2016.

[23] Y. Zhu, L. Xie, and T. Su, "Visualization tests on scour rates below pipelines in steady currents," *Journal of Hydraulic Engineering*, vol. 145, no. 4, Article ID 04019005, 2019.

[24] H. M. Azamathulla and N. A. Zakaria, "Prediction of scour below submerged pipeline crossing a river using ANN," *Water Science and Technology*, vol. 63, no. 10, pp. 2225–2230, 2011.

[25] H. M. Azamathulla, M. A. M. Yusoff, and Z. A. Hasan, "Scour below submerged skewed pipeline," *Journal of Hydrology*, vol. 509, pp. 615–620, 2014.

[26] M. Najafzadeh, G. Barani, and M. R. H. Kermani, "Estimation of pipeline scour due to waves by GMDH," *Journal of Pipeline Systems Engineering and Practice*, vol. 5, no. 3, Article ID 06014002, 2014.

[27] M. Najafzadeh, G. Barani, and H. Azamathulla, "Prediction of pipeline scour depth in clear-water and live-bed conditions using group method of data handling," *Neural Computing and Applications*, vol. 24, no. 3-4, pp. 629–635, 2014.

[28] M. Najafzadeh and F. Saberi-Movahed, "GMDH-GEP to predict free span expansion rates below pipelines under waves," *Marine Georesources & Geotechnology*, vol. 37, no. 3, pp. 375–392, 2019.

[29] M. Najafzadeh and S. Sarkamaryan, "Extraction of optimal equations for evaluation of pipeline scour depth due to currents," *Proceedings of the Institution of Civil Engineers-Maritime Engineering*, vol. 171, no. 1, pp. 1–10, 2018.

[30] W. Park, C. Yoo, D. Shin, T. Kim, and H. Lee, "A study on the risk assessment of river crossing pipeline in urban area," *Journal of the Korean Institute of Gas*, vol. 24, no. 2, pp. 22–28, 2020.

[31] Y. Zhang, S. Zhang, and G. Li, "Seabed scour beneath an unburied pipeline under regular waves," *Marine Georesources & Geotechnology*, vol. 37, no. 10, pp. 1247–1256, 2019.

[32] F.-P. Gao, B. Yang, Y.-X. Wu, and S.-M. Yan, "Steady current induced seabed scour around a vibrating pipeline," *Applied Ocean Research*, vol. 28, no. 5, pp. 291–298, 2006.